Effect of Particle Shape on the Compaction and Flow Properties of Powders

Kazumi DANJO,* Kazutoshi KINOSHITA, Kazutaka KITAGAWA, Kotaro IIDA, Hisakazu SUNADA and Akinobu OTSUKA

Faculty of Pharmacy, Meijo University, Yagoto-Urayama, Tempaku-cho, Tempaku-ku, Nagoya 468, Japan. *Received March 3, 1989*

In order to clarify the effect of particle shape on the mechanical properties of powders, such as compaction and flow, the centrifugal compaction test, the tensile test, the direct shear test and Carr's flowability test were carried out on several kinds of fine powders having various particle shapes. Introducing the concept of "apparent adhesion," the effect of particle shape on the porosity, was examined. It was found that the porosity of a powder bed diminished as the sphericity of the particles increased. The flow properties were also affected by particle shape. With increasing shape factor, the flowability increased.

Keywords particle shape; compaction; porosity; tensile strength; apparent adhesion; repose angle; flowability

It is well known that the mechanical properties of powders, such as adhesion and cohesion properties, compaction properties and flowability, are largely dependent on particle size and shape, surface characteristics, humidity and so on. The effects of particle diameter,[1] humidity[2,3] and temperature[4] on the mechanical properties of powders have been reported. Nikolakakis and Pilpel[5,6] have investigated the effect of particle shape and size on the tensile strength. Ridgway and Rupp,[7] Kawashima *et al.*,[8] and Fukuzawa and Kimura[9] studied the influence of particle shape on the angle of repose and the flow rate. It is generally accepted that the compaction and flow properties of powders deteriorate as the shape of particles becomes more irregular. However, in almost all the studies reported, the samples used were coarse powders. In the case of fine powders, it is supposed that a number of factors should be considered. Such factors include the size or mass of the particle, and the adhesive force between particles, as well as the shape.

In the present study, using several kinds of fine organic and inorganic powders of different particle shapes, measurements of the porosity, tensile strength and flowability of powder beds were carried out and the effect of the particle shape on these properties was examined.

Experimental

Materials Powder samples used are listed in Table I with their physical properties. The true density was measured with a Shimadzu-Micromeritics type 1302 helium-air pycnometer. The Heywood diameter d and particle shape index ψ were determined using at least 1000 particles with an image analyzer (LUZEX 500, Nireco Ltd.). The particle shape index ψ was obtained by dividing the actual projected area of a particle A by the area of a circle having a diameter equivalent to the maximum projected length, ML, as shown in Eq. 1.

$$\psi = 4A/(\pi ML^2) \quad (1)$$

Therefore, the value of particle shape index ψ ranges from zero to 1. The value approaches unity as the sphericity of a particle increases.

The mean particle mass was determined by direct counting of 3000—10000 particles, using a microscope. The counted samples were weighed with a Chyo electronic balance (JPN-180W).

Compaction Procedure in a Centrifugal Field The apparatus consisted of a split cylindrical cell, 50 mm in diameter and 20 mm in depth. The split cell filled with powder was fitted on a rotor driven by a variable-speed electric motor, and spun for 5 min. The powder in the cell packed down and the resulting void was filled with more powder, then the cell was spun again. The operation was repeated untill the apparent volume of powder no longer changed. The weight of powder was determined before the tensile strength measurements and the porosity of the powder bed was calculated. The centrifugal acceleration α was obtained as the product of the distance of the powder bed from the axis of rotation r and the square of the angular velocity of rotation ω.

Tensile Strength Measurements Figure 1 is a skech of the tensile tester for measuring the tensile strength. The split cell was the same one as used in the compaction test described above. One half of the cell is movable on three ball bearing tracks, and the other half cell is fixed to a stand. The operation of the tester was described in the previous paper.[10]

Measurements of Flow Properties of Powder 1) Direct Shear Test: A schematic diagram of the direct shear tester designed by Tsunakawa and Aoki[11] is shown in Fig. 2. The apparatus is of the constant volume type and the shear cell is similar to a Jenike cell (inside diameter 100 mm and

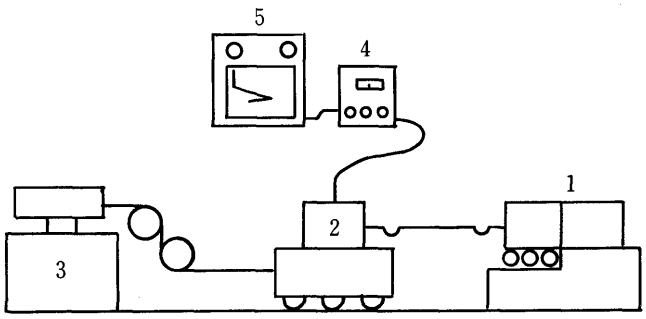

Fig. 1. Schematic Diagram of Apparatus for Measuring Tensile Strength of Powder Bed

1, split cell; 2, strain gauge; 3, motor; 4, amplifier; 5, recorder.

TABLE I. Physical Properties of Powders Used

Material	Density ρ (g/cm^3)	Average particle diameter d (μm)	Average particle mass (μg)	Shape index of particle, ψ
Potato starch	1.48	30.1	2.01×10^{-2}	0.880
α-Lactose monohydrate	1.53	17.5	3.47×10^{-3}	0.651
Calcium carbonate	2.67	18.4	5.05×10^{-3}	0.631
Dibasic calcium phosphate	2.09	15.6	2.24×10^{-3}	0.547
Crystalline cellulose	1.57	38.3	7.93×10^{-3}	0.428
Sodium glutamate	1.53	35.1	5.26×10^{-3}	0.379
Croscarmellose sodium	1.43	38.6	1.55×10^{-2}	0.271

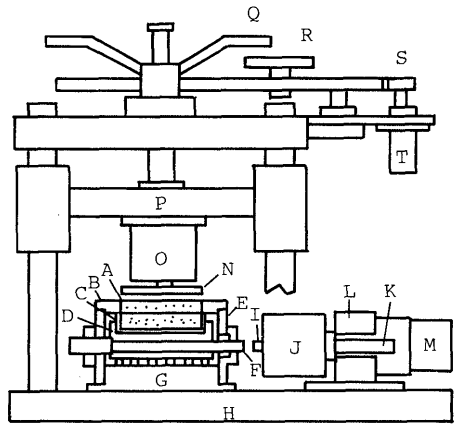

Fig. 2. Schematic Diagram of Direct Shear Tester

A, powder; B, ring; C, metal mold; D, base mold; E, guide ring; F, shaft; G, plate; H, press base; I, loading pin; J, load transducer; K, screw shaft; L, reduction gear; M, syncronous motor; N, lid; O, load transducer; P, arm; Q, R, handle; S, gear; T. speed control motor.

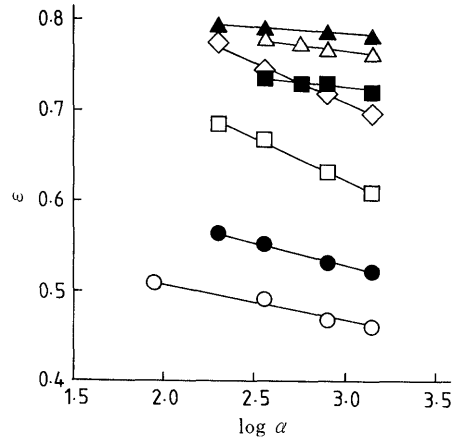

Fig. 3. Relationship between Porosity (ε) and Logarithm of Centrifugal Acceleration ($\log\alpha$)

○, potato starch; □, α-lactose monohydrate; ●, calcium carbonate; ■, dibasic calcium phosphate; △, crystalline cellulose; ◇, sodium glutamate; ▲, croscarmellose sodium.

depth 60 mm), which is horizontally split in half. The upper half cell is screwed to the top of a guide ring, forming the fixed part of the cell. The lower half is inserted into a base mold with a shaft across the center line, forming the movable part of the cell.

The test powder was introduced into the shear cell. The lid was lowered and a normal stress was applied. The synchronous motor was driven keeping the normal stress as constant as possible in the early stage of shearing. The shear stress increased to a critical value indicated by the point E in Fig. 7, where a steady state of failure of the powder bed was reached. Then, the lid was lifted slowly and the shear stress decreased with decreasing normal stress. The height of the sample was measured by using the transducer and strain meter. Each measurement was repeated several times.

2) Flowability Test by Carr's Method: The angle of repose, compressibility, angle of spatula and degree of uniformity coefficient were measured with a powder tester (Hosokawa Micron Co.) and the flowability values *FA* were calculated from the results of the above four tests according to Carr's method.[12]

Results and Discussion

Compaction Properties of Powders The relationship between logarithm of centrifugal acceleration α (abscissa) and the porosity ε (ordinate) for materials of different particle shapes is shown in Fig. 3. The porosity ε decreases with increasing centrifugal acceleration α and a linear relationship is obtained for each powder. However, the value of ε at a given value of α varied widely depending on the material.

Figure 4 shows the relationship between logarithm of centrifugal acceleration α and logarithm of tensile strength T. These plots also give a linear relationship for each powder. In the previous paper,[2,3] we assumed that the porosity of the powder bed was affected by the "apparent adhesion," which was defined as the ratio of the interparticle force H to the external force acting on a particle F. When the value of the adhesive force H is sufficiently large compared to the value of F the particle may stay at the contact point with the neighboring particles, even if vacant spaces exist in the lower layer of the powder bed. As the value of F increases, the probability of a particle falling into the vacant spaces to make the bed more compact will increase. For native and surface-modified quartz powders of different particle sizes and different moisture contents, a fairly good correlation was observed between the logarithm of "apparent adhesion" and $\log(\varepsilon-0.26)$.[3]

In those systems all the samples were similar in shape.

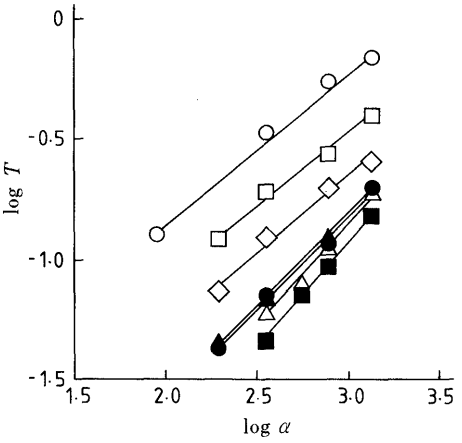

Fig. 4. Relationship between log T and log α

○, potato starch; □, α-lactose monohydrate; ●, calcium carbonate; ■, dibasic calcium phosphate; △, crystalline cellulose; ◇, sodium glutamate; ▲, croscarmellose sodium.

Since powders with a variety of shapes were used in the present study, we attempted to discuss the results using the measured values directly. It is supposed that the adhesive force for one particle is related to the value of the tensile strength of the powder bed T divided by the number of particles per unit cross-sectional area N. The external force acting on a particle is given as the product of the particle mass m and the centrifugal acceleration α. If it is assumed that the value of N is proportional to $(1-\varepsilon)$ and inversely proportional to the average area of the particle (and consequently the square of the particle diameter d^2), the value of $\{d^2Tg/(1-\varepsilon)m\alpha\}$ may be closely related to the ratio of the adhesive force for one particle to the external force acting on the particle, where g is the gravitational acceleration. Plots of $\log\varepsilon$ against $\log\{d^2Tg/(1-\varepsilon)m\alpha\}$ are shown in Fig. 5. A linear relationship was observed for each powder. Then, ε at which $\{d^2Tg/(1-\varepsilon)m\alpha\}$ equals 100 (obtained by interpolation or extrapolation) was plotted against the particle shape index ψ (Fig. 6). It has become apparent that the shape of powder particles plays an important role in the porosity, when the ratio of the adhesive force for one particle to the external force acting

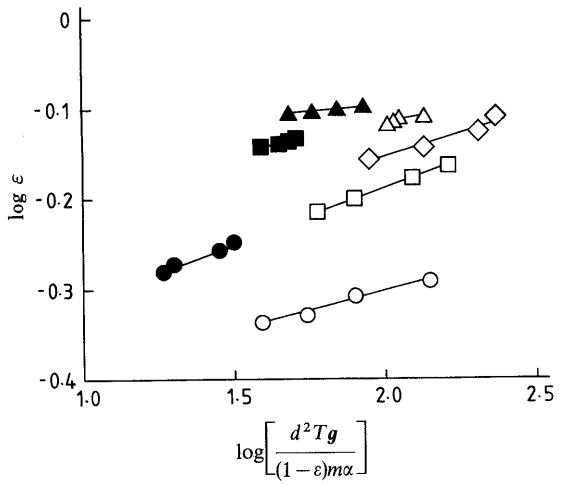

Fig. 5. Relationship between $\log\varepsilon$ and $\log\{d^2Tg/(1-\varepsilon)m\alpha\}$

○, potato starch; □, α-lactose monohydrate; ●, calcium carbonate; ■, dibasic calcium phosphate; △, crystalline cellulose; ◇, sodium glutamate; ▲, croscarmellose sodium.

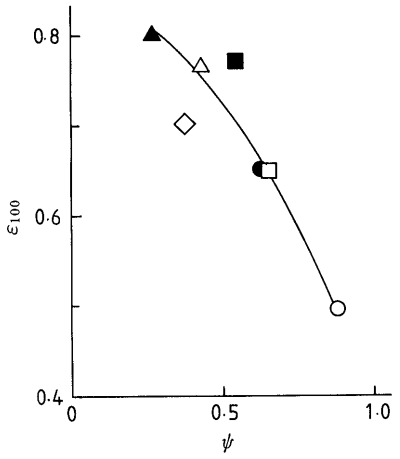

Fig. 6. Effect of Shape Index of Particle (ψ) on the Porosity (ε_{100})

ε_{100}, porosity at which $\{d^2Tg/(1-\varepsilon)m\alpha\}$ equals 100; ○, potato starch; □, α-lactose monohydrate; ●, calcium carbonate; ■, dibasic calcium phosphate; △, crystalline cellulose; ◇, sodium glutamate; ▲, croscarmellose sodium.

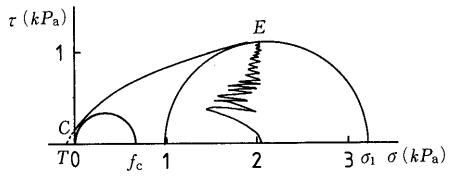

Fig. 7. Typical Yield Loci for Dibasic Calcium Carbonate

on the particle is fixed at a constant value.

Flow Properties of Powders A typical yield locus for dibasic calcium carbonate powder is shown in Fig. 7, where σ_1 is the major consolidation stress, τ is the shear stress and f_c is the unconfined yield stress.

Tsunakawa[13] proposed that the ratio of f_c to $\rho_a g$, which is denoted as *FI*, can be a measure of the flowability of cohesive powders, where ρ_a is the bulk density of the powder. This value corresponds to the maximum height that the powder layer having a unit cross-sectional area is able to stand vertically under the force of gravity. Consequently, the *FI* value should generally decrease as the flowability of powder increases.

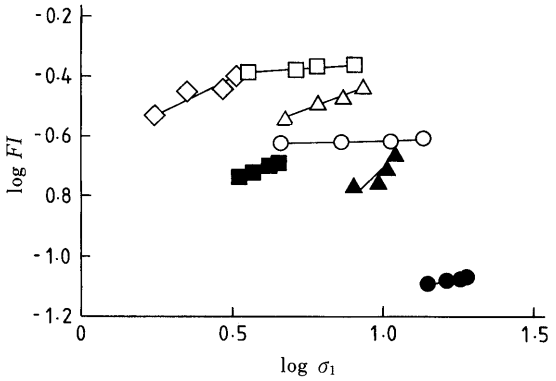

Fig. 8. Relationship between $\log FI$ and $\log\sigma_1$

○, potato starch; □, α-lactose monohydrate; ●, calcium carbonate; ■, dibasic calcium phosphate; △, crystalline cellulose; ◇, sodium glutamate; ▲, croscarmellose sodium.

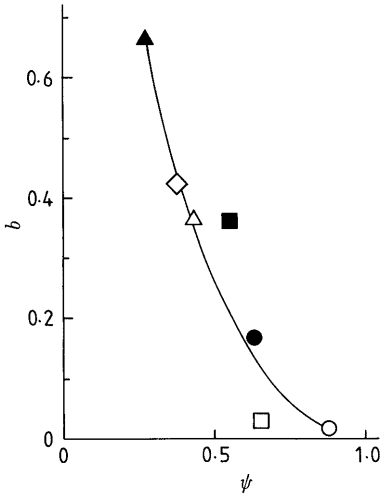

Fig. 9. Effect of Shape Index of Particle ψ on the Constant b

○, potato starch; □, α-lactose monohydrate; ●, calcium carbonate; ■, dibasic calcium phosphate; △, crystalline cellulose; ◇, sodium glutamate; ▲, croscarmellose sodium.

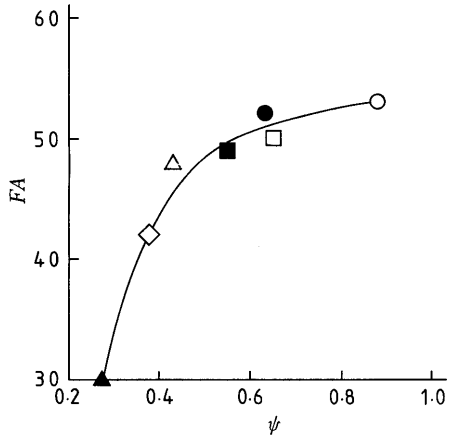

Fig. 10. Effect of Shape Index of Particle ψ on Carr's Flowability *FA*

○, potato starch; □, α-lactose monohydrate; ●, calcium carbonate; ■, dibasic calcium phosphate; △, crystalline cellulose: ◇, sodium glutamate; ▲, croscarmellose sodium.

However, the value of *FI* increases with increasing σ_1, and the following empirical equation was proposed by Tsunakawa[13]:

TABLE II. Flow Properties of Powders in Carr's Test

Material	Angle of repose (°)	Angle of spatula (°)	Compressibility coefficient (%)	Uniformity (units)	Flowability (points)
Potato starch	58.9	68.2	28.5	6.1	53.0
α-Lactose monohydrate	51.0	59.5	48.2	3.8	50.0
Calcium carbonate	52.5	66.2	37.3	2.2	52.0
Dibasic calcium phosphate	54.3	67.8	44.6	3.7	49.0
Crystalline cellulose	53.0	68.1	32.4	18.0	48.0
Sodium glutamate	57.9	69.6	59.5	3.6	42.0
Croscarmellose sodium	67.8	71.9	47.5	15.0	30.0

$$FI = f_c/\rho_a g = a\sigma_1^b \quad (2)$$

where a and b are constants. These two coefficients are considered to be indexes of the flowability of powders.

Figure 8 represents the logarithm of FI as a function of $\log \sigma_1$, and a and b in Eq. 2 can be caluculated for each powder. The relationship between the value of b and the particle shape index ψ is shown in Fig. 9, which indicates that the b value decreases, *i.e.*, flowability increases, as the value of ψ increases.

The data obtained by Carr's flowability measuring method are summarized in Table II.

Figure 10 represents the relationship between Carr's FA value and ψ. The FA value increased with increase in the sphericity of particles, particularly in the region of ψ value from *ca.* 0.3 to 0.5.

In conclusion, it was found that the compaction and flow properties of fine powders were strongly influenced by the particle shape, as in the case of coarse powders.

Acknowledgements We are grateful to Dr. Hiroshi Tsunakawa, Department of Chemical Engineering, Yokohama National University, for designing the shear tester.

References

1) A. Otsuka, K. Danjo and H. Sunada, *Chem. Pharm. Bull.*, **21**, 428 (1973).
2) K. Danjo and A. Otsuka, *Chem. Pharm. Bull.*, **26**, 2705 (1978).
3) A. Otsuka and K. Danjo, *J. Powder & Bulk Solids Technol.*, **3**, 10 (1979).
4) K. Danjo and A. Otsuka, *Chem. Pharm. Bull.*, **36**, 763 (1988).
5) I. Nikolakakis and N. Pilpel, *Powder Technol.*, **45**, 79 (1985).
6) I. Nikolakakis and N. Pilpel, *Powder Technol.*, **56**, 95 (1988).
7) K. Ridgway and R. Rupp, *J. Pharm. Pharmacol.*, **21**, 30S (1969).
8) Y. Kawashima, K. Matsuda and H. Takenaka, *Yakugaku Zasshi*, **92**, 1263 (1972).
9) H. Fukuzawa and S. Kimura, *Yakugaku Zasshi*, **94**, 69 (1974).
10) K. Danjo and A. Otsuka, *Yakugaku Zasshi*, **100**, 893 (1980).
11) H. Tsunakawa and R. Aoki, *Powder Technol.*, **33**, 249 (1982).
12) R. L. Carr, *Chem. Eng.*, **72**, 163 (1965).
13) H. Tsunakawa, *J. Soc. Powder Technol. Jpn.*, **19**, 516 (1982) and **23**, 437 (1986).